# 行政院國家科學委員會專題研究計畫 成果報告

## 提昇鎳基超合金 Inconel 718 切削加工性能與刀具使用壽命之研究

## 研究成果報告(精簡版)

計 畫 類 別 ：個別型
計 畫 編 號 ：NSC 97-2221-E-150-061-
執 行 期 間 ：97 年 08 月 01 日至 98 年 10 月 31 日
執 行 單 位 ：國立虎尾科技大學機械與電腦輔助工程系

計 畫 主 持 人：林盛勇

計畫參與人員：碩士班研究生-兼任助理人員：鄭元祐
碩士班研究生-兼任助理人員：唐啟哲
碩士班研究生-兼任助理人員：林義祥

報 告 附 件 ：出席國際會議研究心得報告及發表論文

處 理 方 式 ：本計畫可公開查詢

中 華 民 國 98 年 12 月 15 日

行政院國家科學委員會補助專題研究計畫成果報告

# 提昇鎳基超合金 Inconel 718 切削加工性能與刀具使用壽命之研究

計畫類別：■個別型計畫　　□整合型計畫

計畫編號：**NSC 97-2221-E-150-061**

執行期間： **97** 年 **8** 月 **1** 日 至 **98** 年 **10** 月 **31** 日

計畫主持人：林盛勇

共同主持人：

計畫參與人員：鄭元祐、唐啟哲、林義祥

執行單位：國立虎尾科技大學 機械與電腦輔助工程系

中　華　民　國　9 8　年　9　月　日

# 行政院國家科學委員會專題研究計畫成果報告

## 提昇鎳基超合金 Inconel 718 切削加工性能與刀具使用壽命之研究

## An investigation on cutting performance and tool life promotion for nickel-based super-alloy Inconel 718 machining

計 畫 編 號：NSC 97-2221-E-150-061
執 行 期 限：97 年 8 月 1 日至 98 年 10 月 31 日
主 持 人：林盛勇 國立虎尾科技大學機械與電腦輔助工程系

## 一、中文摘要

隨著航太科技與生醫科技的蓬勃發展，鎳基超合金等難加工合金的應用也日益廣泛，因其在高溫具有良好機械性質、高強度、高溫耐蝕性。能否高效率加工這些材料，關係到航太、生醫和石化等重要工業的發展速度。因此必須解決切削難加工材所帶來的難題，加快關鍵技術的開發應用，期創造新的加工技術來滿足製造業的需求。

本文使用有限元素法建立一鎳基超合金 Inconel 718 超音波輔助車削模型，藉由此模型之數值模擬探討不同加工參數時工件切削溫度分佈和切削力等變化。實驗方面則是利用超音波輔助並配合液態氮冷卻來車削 Inconel 718，將超音波產生器架設在刀具上，其振動方向為切削切線方向。由動力計所量測的切削力與表面粗糙度輪廓儀量測完成面粗糙度值，進行分析與探討。結果顯示：Inconel 718 車削數值模擬，超音波輔助車削可有效的降低切削力。車削實驗時，利用超音波輔助並配合液態氮冷卻之使用，可降低切削力，對於表面粗糙度也有很大的改善。

**關鍵詞：鎳基超合金 Inconel 718、超音波輔助車削 、液態氮**

## 二、前言

Inconel 718 合金是一種時效硬化的 Fe-Cr-Ni 基變形高溫耐熱超合金，它具有較高的高溫強度、良好的抗氧化性、抗熱腐蝕性、斷裂韌性和疲勞性能，其良好的高溫性能，已被廣泛地運用於火箭發動機、航空飛機及其它航空器的耐熱零件。其對於腐蝕及潛變表現出特別的阻抗，使得它們適用於油品、石化、醫療、太空船、潛艇、核能反應器及蒸汽動力場等。由於 Inconel 718 材料的進步，明顯提升引擎的效率及燃油消耗的降低，先進航空器引擎鎳基合金之重量約佔了 50%，Inconel 718 是這種等級中一種最通用的合金，特別是應用於航太引擎裡的渦輪盤、框、環、葉片及引擎底座之製造。其又適合製造使用於-17~700℃溫度、高腐蝕阻抗及惡劣嚴苛等工作環境之高強度相關零件，如太空船主引擎、航空器結構件、泵浦本體及零件、飛彈零件、低溫儲存槽、熱擠伸模等。目前，該合金亦廣泛被應用於汽車、通訊和電子工業，在高溫合金的用量中占有絕對重要的地位。

本研究針對鎳基超合金材料，利用 Deform-2D 軟體建立一正交切削模型，藉由此模型之數值分析可了解切削力和溫度的變化，並與實驗結果作比較。使用液態氮進行冷卻結合超音波輔助振動切削在不同切削變數與條件組合下進行實驗。利用所量測到的結果，比較在各種切削條件下對切削力和表面粗糙度的影響。此結果將有助於提高實際加工時

成品的尺寸精度和成品品質的改善。

## 三、數值模擬分析

本模擬所選擇的工件材料為鎳基超合金(Inconel 718)，車削過程刀具運動為單一方向，超音波輔助車削模擬模型如圖 1(a)所示，將刀具設為往復運動。工件網格劃分如圖 1(b)所示，工件底部沿 x、y 方向位移完全固定，左側沿 x 方向位移固定。刀具由工件右側水平切入，利用軟體中的網格細化功能，使切削區域網格較密，遠離切削區域網格較疏，這樣安排滿足計算精度的同時減小了計算量。

Inconel 718 車削模擬規劃如表 1 所示，是由 3 種切削速度、3 種進給量、1 種切削寬度和 3 種刀面斜角所組成，共有 3×3×1×3＝27 種組合。Inconel 718 超音波輔助車削模擬規劃如表 2 所示，是由 2 種切削速度、3 種進給量、1 種切削寬度、1 種刀面斜角和 3 種超音波輔助振動頻率所組成，共有 3×3×1×1×3＝27 種組合。

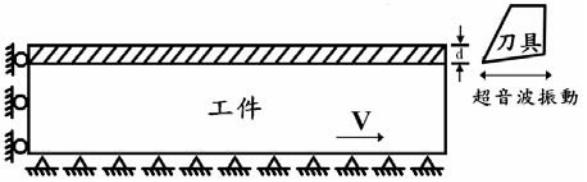


(a)模擬模型及其邊界條件

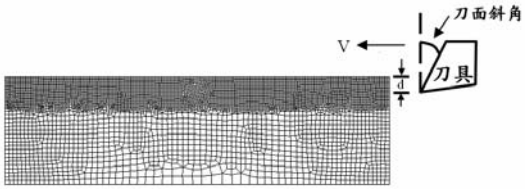


(b)網格分割

圖 1 車削模擬模型示意圖、邊界條件與網格分割

表 1 Inconel 718 傳統車削模擬參數規劃

| | |
|---|---|
| 切削速度 V（m/min） | 125、188、251 |
| 切削深度 d（mm） | 0.06、0.08、0.1 |
| 切削寬度 b（mm） | 1 |
| 刀面斜角 α（deg.） | -10、0、10 |

表 2 Inconel 718 超音波輔助車削模擬參數規劃

| | |
|---|---|
| 切削速度 V（m/min） | 125、188 |
| 切削深度 d（mm） | 0.06、0.08、0.1 |
| 切削寬度 b（mm） | 1 |
| 超音波輔助振動頻率（kHz） | 0、10、20 |
| 振幅（μm） | 5 |
| 刀面斜角 α （deg） | 0 |

## 四、實驗方法與規劃

本實驗以車削 Inconel 718 鎳基超合金為主題，參考所研讀過的文獻中，採用其建議加工 Inconel 718 的參數範圍，以深冷液體液態氮(-196℃)做為切削液，並加入超音波輔助，觀察對於切削力、表面粗糙度和刀具磨耗的影響。

車削變數與條件如表 3 所示，是由 2 種主軸轉速、3 種進給量、3 種切削深度和有/無使用超音波輔助所組成，共有 2×3×3×2=36 種組合。進行全因子實驗，利用實驗所量測到的結果，比較在各種切削條件下對切削力、表面粗糙度和刀具磨耗的影響。

表 3 超音波輔助車削實驗參數規劃

| | |
|---|---|
| 切削速度 V（m/min） | 125、188 |
| 進給率 f（mm/rev） | 0.06、0.08、0.1 |
| 徑向切削深度（mm） | 0.1、0.15、0.2 |
| 超音波輔助頻率（切線方向）(kHz) | 0、20 |
| 切削液 | 液態氮 |

本實驗車刀刀具採用 SECO CBN10 捨棄式刀片及明和公司所生產製造之超音波產生器。車床型號為勝傑公司 SJ-510×1000GW，主軸最高轉速 1500rpm，熱影像分析儀使用美國 FLUKE 公司製造，型號為 Ti45，最小對焦距離 0.15 米，檢測數據採集/圖像頻率 30/60Hz，溫度測量範圍-20℃ 至 1200℃，精度±

2°C 或 2%，發射率修正 0.1 至 1.0( 0.01 增量 )。本實驗儀器架設與配置如圖 2 所示。

（a）實驗儀器配置現場圖

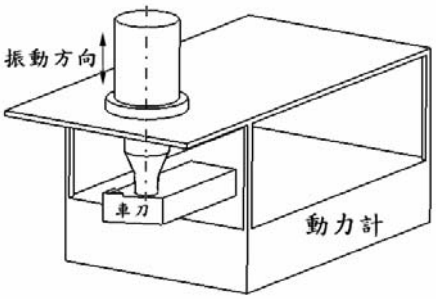


（b）超音波振動架設示意圖

（c）熱影像分析儀

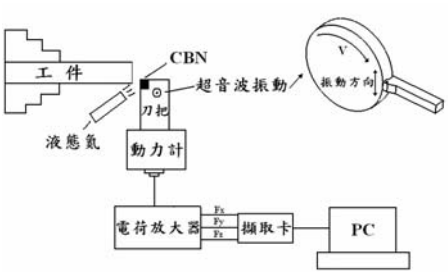


（d）實驗儀器配置示意圖

圖 2 Inconel 718 超音波輔助車削實驗熱影像分析儀與相關儀器架設配置

## 五、結果與討論

### 5.1 模擬與實驗結果之驗證

圖 3 顯示於切削速度 125m/min、徑向切削深度 0.1mm，不同進給率切線方向切削力分量數值模擬與實驗結果之比對。此比較驗證發現此二者的結果相當接近，證實本車削數值模擬預測模型是正確且可行的。

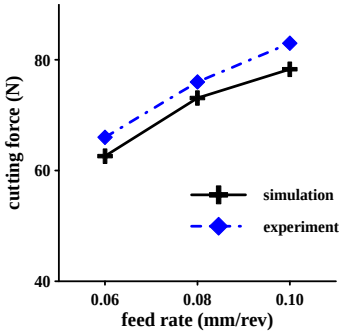


圖 3 切削速度 125m/min 徑向切削深度 0.1mm 與不同進給率時，切線方向之切削力數值模擬與實驗結果比對

### 5.2 模擬結果與分析

由圖 4 的結果可比較出在傳統車削時，不同的參數其切線方向切削力分量的大小，切削力會隨著切削速度的增加而降低，刀面斜角為負的時，切削力最大。觀察圖 5 的結果可看出超音波輔助車削其切削力所呈現的規律性和傳統車削一樣，切削力會隨著切削速度的增加而降低。超音波輔助車削切削力的值會比傳統車削時低，且振動頻率越大，切削力越小。因此發現加入超音波輔助車削可有效的降低切削力。

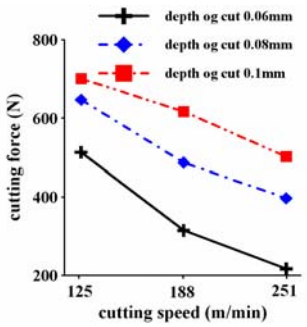


（a）刀面斜角 10°

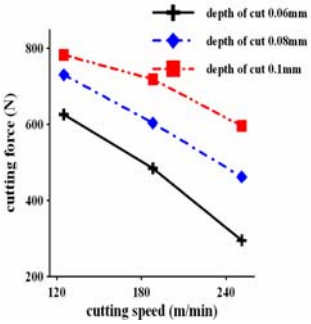


（b）刀面斜角 0°

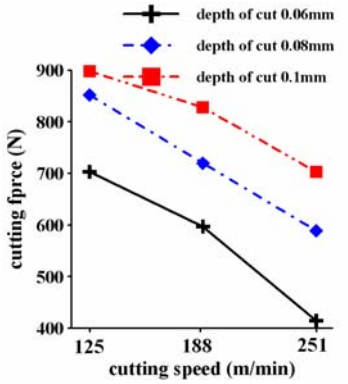


（c）刀面斜角-10°

圖 4 傳統車削不同刀面斜角與切削深度切線方向切削力分量與切削速度之關係

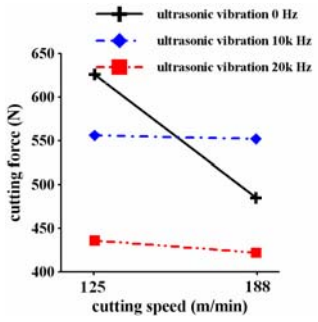


（a）切削深度 0.06mm

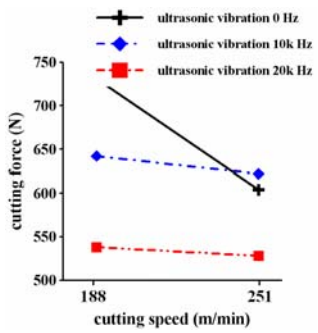


（b）切削深度 0.08mm

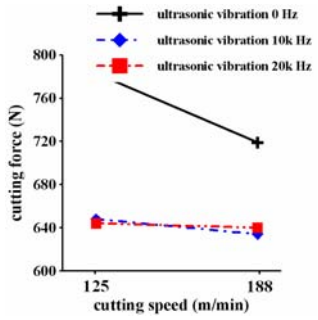


（c）切削深度 0.1mm

圖 5 超音波輔助車削不同切削深度與振動頻率切線方向切削力分量與切削速度之關係

在切削初始階段時，切削溫度上升的較為快速，隨著切削的進行，溫度逐漸進入穩定的狀態。圖 6、7 可以看出隨著切削速度和切削深度的增加，其切屑和刀刃溫度就越高。

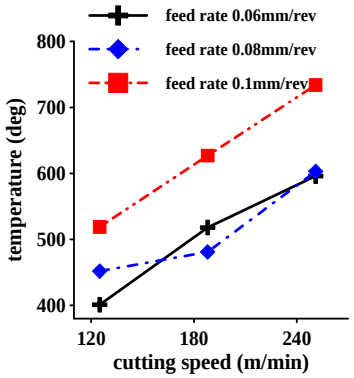


圖 6 不同切削深度切屑最高溫度與切削速度之關係

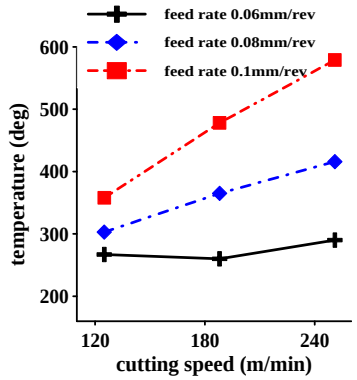


圖 7 不同切削深度刀刃附近的溫度與切削速度之關係

### 5.3 實驗量測結果與分析

本車削實驗共量測了 36 組實驗數據，以液態氮作為冷卻液，分析探討有無使用超音波輔助車削對於切削力、表面粗糙度及刀具磨耗的影響與溫度的變化情形。

本實驗將所量測到的三個軸向分量(切線方向、軸向、徑向)進行向量相加為切削合力，由圖 8、9 可看出其規律性。在傳統車削和超音波輔助車削情況下，切削力會隨著切削速度的增加而降低；隨著切削深度和進給率的增加而增加。由所得到的結果數據相互比較，發現傳統車削時切削力比超音波輔助車削時切削合力來的大，利用上述結果得知超音波輔助可以有效的降低切削力。

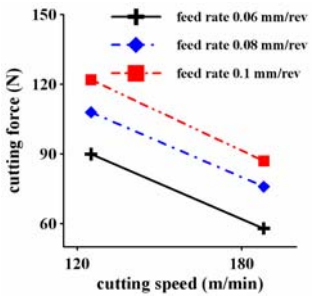


(a)徑向切深 0.1mm

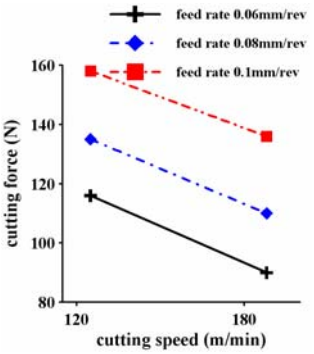


(b)徑向切深 0.15mm

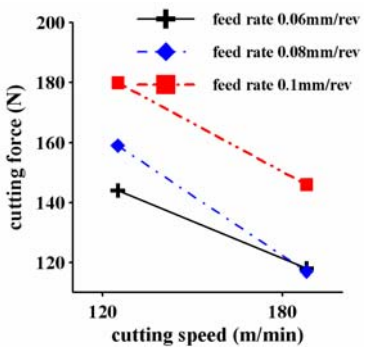


(c)徑向切深 0.2mm

圖 8 傳統車削不同徑向切深與進給率切削合力與切削速度之關係

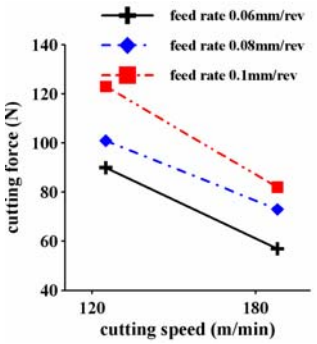


(a)徑向切深 0.1mm

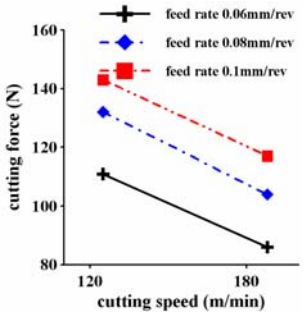


(b)徑向切深 0.15mm

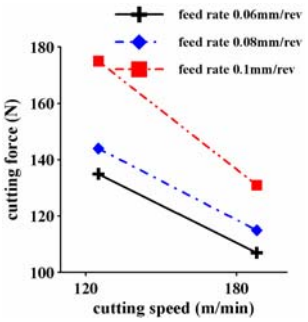


(c)徑向切深 0.2mm

圖 9 超音波輔助車削不同徑向切深與進給率切削合力與切削速度之關係

由圖 10 和 11 可看出在傳統車削，表面粗糙度值會隨著徑向切深的增加而增加。在徑向切深 0.1mm 和 0.15mm 時，表面粗糙度值會隨著切削速度的增加而降低，隨著進給率的增加而增加；但徑向切深 0.2mm 時，表面粗糙度值會隨著切削速度的增加而增加。在切削速度 188m/min、進給量為 0.06mm/rev 和徑向切深為 0.1mm 時，可以獲得較好的表面粗糙度。而在超音波輔助車削，表面粗糙度值會隨著切削速度和徑向切深的增加而降低，隨著進給率的增加而增加。在切削速度 188m/min、進給量為 0.06mm/rev 和徑向切深為 0.2mm 時，可以獲得較好的表面粗糙度。

經由表 4、5 結果數據比較顯示，在切削速度 125m/min 時，使用超音波輔助對表面粗糙度值改善率為 0%~25%；在切削速度 188m/min 時，使用超音波輔助對表面粗糙度值改善率 20%~61%。由此數據顯示使用超音波輔助車削加上切速的提升對於表面粗糙度有極大的改善。

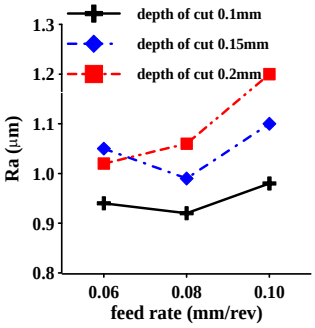


(a)切削速度 125m/min

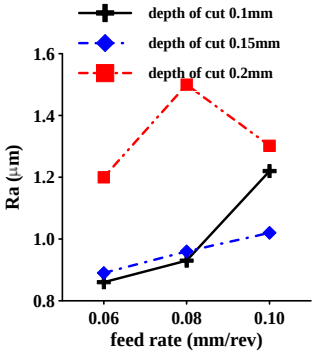


(b)切削速度 188m/min

圖 10 傳統車削不同切削速度表與切削深度面粗糙度與進給率之關係

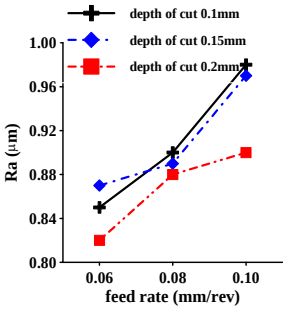


(a)切削速度 125m/min

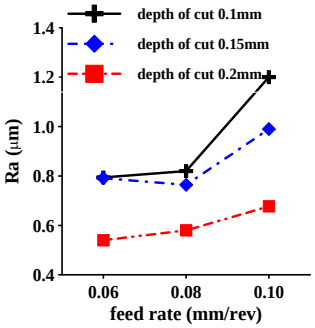


(b)切削速度 188m/min

圖 11 超音波輔助車削不同切削速度與切削深度表面粗糙度與進給率之關係

表 4 切削速度 125m/min，有無使用超音波輔助對表面粗糙度值之改善率

| 切削速度 (m/min) | 進給率 (mm/rev) | 徑向切深 (mm) | 超音波輔助 | 表面粗糙度值 (μm) | 改善率 |
|---|---|---|---|---|---|
| 125 | 0.1 | 0.2 | 無 | 1.2 | 25% |
| 125 | 0.1 | 0.2 | 有 | 0.9 | |
| 125 | 0.1 | 0.1 | 無 | 0.98 | 0% |
| 125 | 0.1 | 0.1 | 有 | 0.98 | |

表 5 切削速度 188m/min，有無使用超音波輔助對表面粗糙度值之改善率

| 切削速度 (m/min) | 進給率 (mm/rev) | 徑向切深 (mm) | 超音波輔助 | 表面粗糙度值 (μm) | 改善率 |
|---|---|---|---|---|---|
| 188 | 0.1 | 0.2 | 無 | 1.5 | 61% |
| 188 | 0.1 | 0.2 | 有 | 0.58 | |
| 188 | 0.1 | 0.1 | 無 | 1.22 | 2% |
| 188 | 0.1 | 0.1 | 有 | 1.2 | |

刀面凹陷磨耗和刀腹磨耗的磨耗情況如圖 12、13 所示，由結果看出在任何加工參數下都會產生此兩種磨耗。凹陷磨耗分別是以凹陷寬度 KB 和凹陷深度 KT 來表示。傳統車削和超音波輔助車削凹陷磨耗的比較如圖 14、15 所示，傳統車削其刀面凹陷磨耗較超音波輔助車削嚴重。傳統車削在較大徑向切深、進給率 0.08 mm/rev ，凹陷磨耗較為嚴重。超音波輔助車削則是在較高進給率（0.1mm/rev）時，凹陷磨耗較為嚴重。

（a）刀尖角落

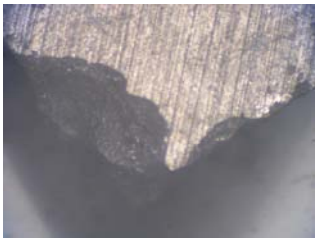

（b）刀面

圖 12 傳統車削在切削速度 125m/min 徑向切深 0.2mm 時，進給率 0.08mm/rev 下刀尖角落和刀面的磨耗狀況

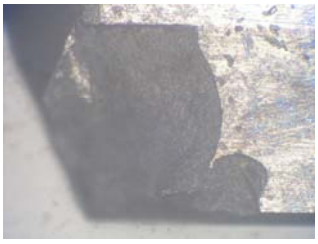

（a）刀尖角落

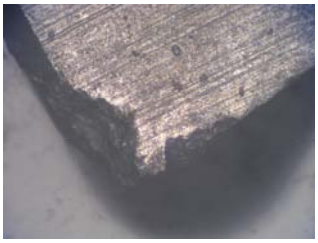

（b）刀面

圖 13 超音波輔助車削在切削速度 125m/min 徑向切深 0.2mm 時，不同的進給率下刀尖角落和刀面的磨耗狀況

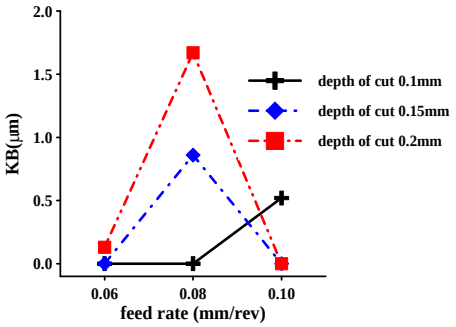


（a）凹陷寬度

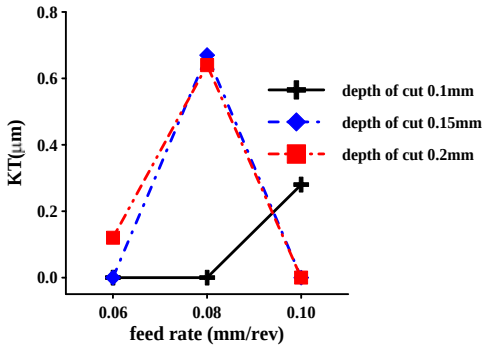


（b）凹陷深度

圖 14 傳統車削不同切削深度與進給率刀面凹陷磨耗大小

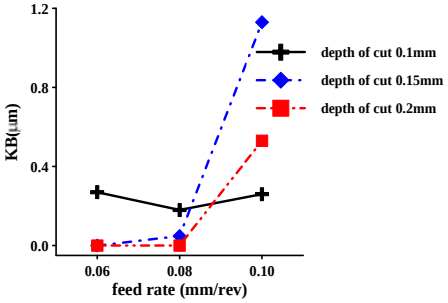


（a）凹陷寬度

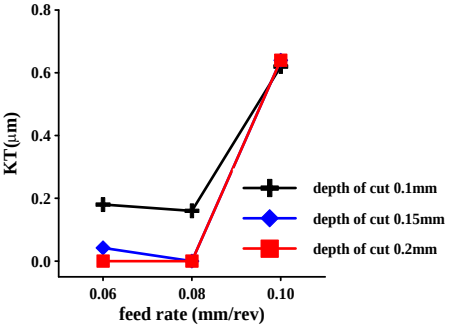


（b）凹陷深度

圖 15 超音波輔助車削不同切削深度與進給率刀面凹陷磨耗大小

由圖 16 和 17 觀察結果發現，超音波輔助車削切削溫度隨切削速度和切削深度的增加而上升。被加工物件因溫度提高而軟化，使得在切削過程中會變的較易切削，工件的軟化進而影響到刀具的壽命，此舉可提升刀具壽命和改善加工品質。由圖 17(b)等高線可以區分溫度的不同區域，綠色和藍色溫度介於 180℃~420℃，而黃色和紅色溫度介於 420℃~600℃之間。切削區域刀刃部位-工件接觸介面的顏色分佈為紅色，其餘工件部份為綠色或是藍色，由圖明白看出最高溫發生在刀刃

上，這些圖十字點位置為溫度最高點座落於刀刃上。


(a) 切削深度 0.1mm

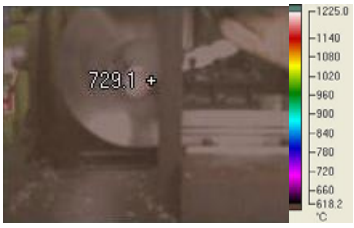


(b) 切削深度 0.15mm


(c) 切削深度 0.2mm

圖 16 切削速度 188m/min 與進給率 0.06mm/rev 超音波輔助車削不同切削深度切削溫度分佈

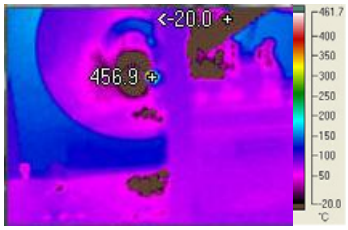


(a) 切削深度 0.1mm

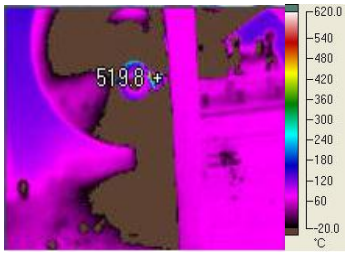


(b) 切削深度 0.15mm


(c) 切削深度 0.2mm

圖 17 切削速度 125m/min 與進給率 0.06mm/rev 超音波輔助車削不同切削深度切削溫度分佈

在車削 Inconel 718 鎳基超合金時，比較有無使用超音波輔助時，結果發現切削速度 125m/min 時，有無超音波輔助溫度的變化不大如圖 18、19 所示。切削速度在 188m/min 時，溫度已有明顯的上升，因本研究搭配超音波輔助車削的激振，刀具與工件間高速接觸相互作用，使溫度極速上升促使工件部份軟化，較易進行切削加工，進而改善刀具壽命和加工件品質。

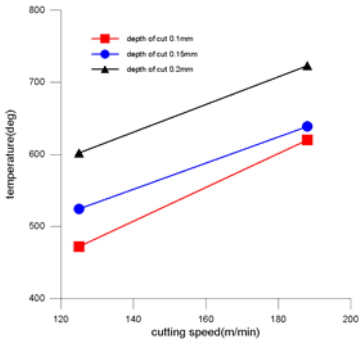


圖 18 無超音波輔助不同切削深度刀刃附近的溫度與切削速度之關係

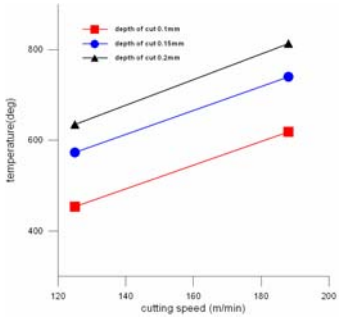


圖 19 有超音波輔助不同切削深度刀刃附近的溫度與切削速度之關係

## 六、結論

本文針對難切削材料建立了描述切削過程的有限元素模型，同時模擬切屑的形成，並透過車削實驗進行驗證，以探討不同切削參數對切削溫度、切削力與刀具磨耗之影響。綜合以上之分析與討論可得到以下之結論：

1. 由 Inconel 718 車削實驗結果與模擬結果作比對，發現兩者切削力大小是相當接近的。本文所發展的模型可以有效預測實驗切削力的大小。
2. 模擬 Inconel 718 車削時，發現在較高進給率時，較容易產生鋸齒狀切屑。切削力方面，隨著振動頻率的增加，切削力降低。證實利用超音波輔助車削可有效的降低切削力。
3. 在 Inconel 718 車削實驗中，使用液態氮來進行冷卻，它能有效降低加工時的切削溫度，減緩刀具的磨損，進而降低車削時的切削力和工件完成表面粗糙度值。利用超音波輔助車削能有效的降低切削力，對於表面粗糙度也有極大的改善。
4. 比較 Inconel 718 傳統車削和超音波輔助車削，刀面主要磨耗型態為凹陷磨耗。傳統車削刀面凹陷磨耗較超音波輔助車削嚴重。

## 七、參考文獻


[1] N. Ahmed, A.V. Mitrofanov, V.I. Babitsky, V.V. Silberschmidt, 2006, Analysis of material response to ultrasonic vibration loading in turning Inconel 718, Materials Science and Engineering A, Vol.424, pp.318-325.

[2] A.V. Mitrofanov, V.I. Babitsky, V.V. Silberschmidt, 2004, Finite element analysis of ultrasonically assisted turning of Inconel 718, J. Mater. Process. Technol., Vol.153-154, pp.233-239.

[3] Z.Y. Wang, K.P. Rajurkar, J. Fan, S. Lei, Y.C. Shin, G.. Petrescu, 2004, Hybrid machining of Inconel 718, Int. J. Mach. Tools Manuf., Vol.43, pp.1391-1396.

[4] T. Kitagawa, A. Kubo and K. Maekawa, 1997, Temperature and wear of cutting tools in high-speed machining of Inconel 718 and Ti-6Al-6V-2Sn, Wear, Vol.202, pp.142-148

[5] E. Z. Li, H. Zeng and X. Q. Chen, 2006, An experimental study of tool wear and cutting force variation in the end milling of Inconel 718 with coated carbide inserts, Journal of Materials Processing Technology, Vol.180, pp.296–304

[6] Altin, M. Nalbant and A. Taskesen, 2007, The effects of cutting speed on tool wear and tool life when machining Inconel 718 with ceramic tools, Materials and Design, Vol.28, pp.2518–2522

[7] E. Kose, A. Kurt and U. Seker, 2008, The effects of the feed rate on the cutting tool stresses in machining of Inconel 718, Journal of Materials Processing Technology, Vol.196, pp.165–173

# 行政院國家科學委員會補助國內專家學者出席國際學術會議報告

97 年　11 月　10 日

| | | | |
|---|---|---|---|
| 報告人姓名 | 林盛勇 | 服務機構及職稱 | 國立虎尾科技大學機械與電腦輔助工程系 教授 |
| 會議時間<br>會議地點 | 97/11/2~97/11/5<br>Kingdom of Bahrain, Manama | 本會核定計畫編號 | NSC 97-2221-E-150-061 |
| 會議名稱 | （中文）先進材料與製程技術國際研討會(AMPT 2008)<br>（英文）The International Conference on Advances in Materials and Processing Technology (AMPT 2008) | | |
| 發表論文題目 | （中文）PCBN 端銑削精密模具車削性能之研究<br>（英文）Performance investigation for precision mold turning by PCBN tool | | |

(一)會議時間與地點:

97年11月2日至5日，於巴林共和國(Kingdom of Bahrain)，Manama (Gulf International Convention Centre，Gulf Hotel)。

(二)會議過程:

由於國內沒有飛機直飛巴林共和國，因此本人於97年11月2日，13:05 搭乘國泰CX511 班機由桃園國際機場先飛至香港，再於14:30 搭乘國泰CX733 班機由香港國際機場飛至巴林共和國。因巴林共和國與台灣有5小時的時差，故到達巴林共和國的Ramee旅館check-in 時，已是97年11月2日22時。

97年11月3日上午8:00，搭上由旅館到會場之大會交通巴士，開始整整三天的議程。11月6日下午15:35 搭乘國泰CX746 的班機由巴林共和國國際機場先飛至杜拜,再原機於16:30 由杜拜國際機場飛至香港，並於97年11月7日上午8:50 搭乘國泰CX460 班機由香港國際機場飛抵至桃園國際機場返台。

(三)會議內容：

大會於11月3日上午8:30開幕，隨後大會分別於11月3日與11月5日安排共9場的專題演講。會中第一場報告邀請A. Gross 博士作專題演講。A. Gross 博士針對未來材料的發展與應用，做了一場很精闢的介紹。會中第二場報告邀請F.A. Al-Sulaiman 教授作專題演講。F.A. Al-Sulaiman 教授演說的題目是先進製造技術於區域性需求之評估。由於沙烏地阿拉伯是一個產油的國家，需要利用大量的管路將原油輸送至不同的地方。因此原油輸送管線的焊接技術，在沙烏地阿拉伯就顯得非常的重

要。同時F.A. Al-Sulaiman 教授目前亦是沙烏地阿拉伯KFUPM的副總裁。第三場報告是邀請清華大學的H. Hocheng 教授作專題演講，H. Hocheng 教授利用細菌對氧化鐵作特定的材料移除，這是一個利用微生物來對氧化鐵進行微加工的研究，令在場與會的學者感到非常的有趣。同時，H. Hocheng教授也是唯一受邀專題演講的台灣學者。會中第四場報告邀請H.J. Al-Zahrani 先生作專題演講。H.J. Al-Zahrani 先生是沙烏地阿拉伯專案管理的總經理。H.J. Al-Zahrani 先生針對碳氫化合物結構材料於材料工程所扮演的腳色，提出其專業的論述。會中第五場報告邀請L.A. Dobrzanski教授作專題演講。L.A. Dobrzanski教授的專長在雷射銲接的加工，此次專題演講其針對鎂合金焊接、刀具燒結與鍍膜技術，做了一場很精闢的介紹。會中第六場報告邀請B. Emin 教授作專題演講。B. Emin 教授發表肥粒晶粒成長於焊接加工中，對空隙自由鋼的影響。會中第七場報告邀請沙烏地阿拉伯Aramco公司的O. A. Hamid 博士作專題演講。O. A. Hamid 博士就先進材料對石油與天然氣的挑戰與機會，進行一場精闢的報告。目前在沙烏地阿拉伯運送石油的管材，已經逐漸被先進的塑膠材料所取代。先進的塑膠材料不僅可降低施工的成本，而且在維修方面也有其方便性。會中第八場報告邀請M. Sarwar 教授作多點切削刀具優勢對先進表面工程的發展之專題演講。利用先進的鍍膜技術於單點或多點切削刀具上鍍膜，可提升刀具的使用壽命、工件的表面精度與提高生產力。會中第九場報告邀請A.M.S. Hamouda 教授作專題演講。雖然鋁、鐵、銅、鎳等金屬合金已廣泛被應用在石油與天然氣工業上，其主要原因係金屬合金具有抗腐蝕、輕量與強度高的優點。然而現今複合材料應用在石油與天然氣工業上，已是未來發展應用的趨勢。

在這次先進材料與製程技術的研討會發表論文篇數中，其中以中東地區國家、台灣及韓國發表的論文篇數最多，而大陸、馬來西亞、日本、美國、澳洲、英國、法國、西班牙、波蘭及印度等國亦有論文發表。由於此次研討會接受的口頭發表論文太多，因此大會共分六個平行場次展開分組討論，每個場次有4-6篇的論文，計五十四場次，共三百二十篇論文，研討論文主題涵蓋材料成形製程、材料移除製程、材料添加製程、CAD/CAM/CAE於材料製程、分析與數值方法應用在材料製程技術、複合與塑膠材料製程、微奈米建構材料製程與技術、材料結合等，是謂國際學術會議中，專注於先進材料與製程議題之難得文獻。本人於11月4日下午擔任材料移除session主持人，隨後於同場地發表本次研討會所投稿之論文，獲得與會學者之肯定，並交換心得與經驗。相關深具價值之論文甚多，不及一一贅述。與會期間，本人也碰到多位來自臺灣的學者，也與日本、韓國、美國、英國、澳洲與大陸學者交談。但是從一些與會學者參與活動之熱絡程度來看，本人發現奈米材料與非

傳統加工仍是目前最熱門的二個研究主題。藉由這次的學術活動交流，使本人更加堅定自己的研究目標與方向，希望下次還有機會參與相關的學術活動。此外，駐巴林共和國的薩代表與丁參事，聞悉此次國際會議有許多來自台灣的教授參加，並相約11月5日下午5時研討會結束後於Gulf Hotel大廳見面。薩代表與丁參事分別說明台灣在巴林共和國的重要性與處境，並期望台灣學術單位能夠搭起外交的橋樑，多與巴林共和國的學術研究單位進行實質性學術交流。同時與會的教授們也向薩代表與丁參事反應辦理巴林共和國簽證的問題，也獲得薩代表與丁參事的允諾。從這件事情當中，我發現台灣的外交困境與外交人員的努力不懈。

(四)攜回大會論文集與摘要各一份

# Performance investigation for precision mold turning by PCBN tool

S. Y. Lin, C. C. Tang, J. C. Shih and S. S. Chi
Department of Mechanical and Computer-Aided Engineering, National Formosa University,
64, Wunhua Rd., Huwei, Yunlin 632, Taiwan; e-mail: sylin@nfu.edu.tw

## ABSTRACT

In order to understand the superior characteristics of PCBN tool for hardened material cutting, to promote the performance and efficiency of molds manufacturing via the high speed machining technology, to investigate the wear mechanism of the tool and the dimensional accuracy and surface finish of the machined molds. SKD11 die steel and polycrystalline cubic boron nitride are used in this study as the workpiece and tool materials, respectively in the turning experiments for investigating the performance of mold manufacturing. Furthermore, in order to reduce the number of experiments, an orthogonal array from the Taguchi's experimental method was utilized to design the sets of cutting conditions, the tool wear was measured through the toolmaker's microscope and the roughness of the machined surface was measured by the roughness measuring instruments after some proper surface layers removed from the workpiece in the experiment to take the associated sampling data prepared for training pattern of the neural network. Besides, the noise-mediator was used to detect cutting noise during each surface layer workpiece removing for the performance judgment of the machining processes. An assessment model of cutting process will be developed using a neural network system if the reliable and sufficient data is taken from the experiments. Based on the developed neural network, the complicated relationships between the cutting parameters (cutting speed, depth of cut and feed rate) and the cutting performance (surface roughness, tool wear and cutting temperature) can be clearly clarified. The best surface roughness of Ra0.29μm is found from the experiments under the cutting conditions of d =0.2mm, f =0.05mm/rev and V=120m/min. This surface quality is equivalent to CMP manufacturing process, the surface roughness of Ra0.2~0.5μm may be attained with that skill. The CMP is always applied to high precision surface processing such as the valve piping and connector components for semiconductor/LED manufacturing.

**KEYWORDS**：PCBN tool, hardened material, tool wear, machined surface finish

## 1. Introduction

Traditionally, the machining of hardened steel (45-65HRC) components has been the domain of grinding operations. Hence, lack of machining efficiency and process flexibility. However, high chromium hardfacing materials are widely used in industry due to its excellent wear resistance. The wear resistance of these materials was mainly achieved by a high hardness and high carbide contents and this makes machining of these hardfacing materials extremely difficult. The development of ultra-hard CBN and PCBN materials have opened up the possibility to machine these materials by turning or milling instead of grinding, and this has offered great improvement of the manufacturing process of hardfaced component in terms of high productivity, flexibility, cost reduction, etc. Cubic boron nitride (CBN) is the second hardest material in the world and PCBN tools have found application in machining of a large range of hard ferrous materials including hardened steel, cast iron and Co/Ni based alloys, etc. PCBN tools are used in machining operations, where tight dimensional tolerances are required due to their elasticity modulus and hardness and low expansion volumetric coefficient. In the last years, PCBN tools were used on shop floors in high speed machining of gray cast iron, white cast iron and hardened steels with low machining costs per piece.

Neo el al. [1] explored the feasibility of using PCBN tools for direct ultra-precision machining of alloy steel. The performance characteristics in terms of surface roughness and tool wear of PCBN and conventional binderless CBN under different machining conditions were studied and their results were compared. Based on the experimental results, PCBN has been found to perform better in terms of wear resistance compared to conventional CBN tool. It is also able to achieve near mirror finish of less than 30 nm$R_a$ and hence it appears to be a promising tool for direct cutting of die and mold materials. Ren et al. [2, 3] used the quick-stop method to study the chip formation of typical hardfacing materials; the deformation behavior of large chromium carbides and their effects on the chip formation process of the workpiece were investigated by examining the chip root obtained and the subsurface of the transient plane. PCBN tool wear modes were revealed using scanning electron microscope and the effect of cutting parameters were also studied by performing series of tests. It was found that the machining process has involved fracture of large carbides ahead of the cutting edge and bending and cracking of the carbide underneath the transient surface. The main modes of tool wear were identified as edge chipping and flank wear, and mechanical loading and the abrasiveness of the carbide particle were the main cause. Furthermore, cutting temperatures of two typical hardfacing materials were studied using remote thermocouple technique and finite element simulation. The effect of microstructure and machining parameters on the cutting temperatures were comparatively investigated using titanium alloy as a reference material. The average cutting temperatures of the hardfacings were found to be ranged from 600 to 700℃ and increased with higher cutting speed and feed rate. A hardfacing with large carbide grains showed lower cutting temperatures and exhibited lower increase rate with cutting speed and feed rate. Liew et al. [4] carried out experiments to investigate the wear mechanism of various grades of PCBN tool in the ultra-precision machining of modified AISI 420 stainless steel at low speeds and depths of cut. The experimental results show that the formation and extent of the surface fracture on the rake face of the PCBN tools are greatly dependent on the cutting forces and the severity of abrasion which are governed by the cutting temperature. The porosity, ductility and the bonding strength of the grains in the tool, apart from its thermal conductivity appear to have great influences on the fracture resistance of the tool. Benga and Abrao [5] dealt with the machinability of hardened 100Cr6 bearing steel when continuous dry turning using mixed alumina, whisker reinforced alumina and PCBN inserts. The experimental results show that cutting speed is the factor which most affects tool life, the factor with the higher significance on the surface roughness value is feed rate and PCBN cutting tools provide longer life than ceramics. Kato et al. [6] explored the improvement of processing efficiency in the high-speed milling of gray cast iron. The cutting performance and wear mechanism of a binderless PCBN tool in practical milling was investigated. It was clarified that the binderless PCBN tool can improve tool life in high-speed milling. Also, the edge shape of the binderless PCBN tool remains sharp in comparison with that of usual PCBN tool, and an excellent low degree of roughness of the machined surface was obtained. Zhou et al. [7] presented a study of the effect of chamfer angle on tool wear of PCBN cutting tool in the super finishing hard turning. The correlation between cutting force, tool wear and tool life were investigated. The optimal chamfer angle for PCBN cutting tool was suggested. Also, the distribution of stresses and maximum principal stress

working on the tool edge were calculated with the use of finite element method. Cook and Bossom [8] explored the current trends in the fabrication and application of PCD and PCBN tools and discussed the more recent and likely future developments to take place in raw material terms. Jr. et al. [9] used two face milling cutter system in high speed cutting of gray cast iron under cutting condition encountered in shop floor. The first system has 24 $Si_3N_4$ ceramic inserts all with square wiper edges. The second system is a mixed tool material system, having 24 wiper inserts, 20 of them are $Si_3N_4$ intercalated by four PCBN inserts. Surface roughness and waviness, tool life and burr formation were the parameters considered to compare the two systems. The second system presented better performance according to all parameters. Wang et al. [10] presented a technique for machining advanced ceramics with liquid nitrogen (LN) cooled PCBN tool, which has been designed to control the cutting tool temperature. The tool wear during the machining of $Si_3N_4$ reduced significantly and the surface roughness was about six times better than normal cutting with LN cooling. The wear on the tool was mainly attrition wear and abrasive wear. Cutting temperature and tool wear in the high-speed machining of aerospace materials, such as Inconel718 and Ti-6Al-6V-2Sn alloys, have been investigated [11] by means of cutting experiments and numerical analysis. It indicates that the tool wear is developed by an abrasive process rather than by a thermally activated mechanism. El-wardany et al. [12] dealt with an experimental and analytical investigation into the different factors which influence the temperature distribution on ceramic tool rake face during machining of difficult-to-cut materials. Temperature measurements on the tool rake were verified using the predictions of the finite element analysis. Experiments were performed to study the effect of cutting parameters, different tool geometries, tool conditions, and workpiece materials on the cutting edge temperatures. Sutter et al. [13] designed a new high-speed machining experiment to obtain orthogonal cutting in a wide range of cutting speeds up to 100m/s. The measurement of the longitudinal cutting force reveals the existence of an optimal cutting speed for which the energy consumption is minimum. The genuine tool-workpiece material interaction can be analyzed with that experimental device.

The effective hardness range for hardened steel machining with PCBN is HRC45-70, due to the superior characteristics of this cutting tool such as excellent wear durability, good thermal resistance and stability, and it is unlikely to generate chemical reactions with the workpiece at high temperature. The hardened material cutting principle is through the large amount of heat generating at the cutting zone which in turn softens the workpiece material at a temperature of 700-800℃ state, the softened material is then easily removed by the PCBN tool. Therefore, long cutting tool life can be still kept as compared to the other cutting tool materials used in hardened workpiece material machining.

## 2. Eexperiment planning

The cutting tool used for turning experiment is PCBN material with a throw-away insert of triangular shape while the workpiece material is mold steel of SKD61 with a heat treatment to 60HRC in hardness. Three process variables related to hard material turning, i.e. depth of cut, cutting speed and feed rate are selected in this study. The former one of these variables was set at three levels, i.e. 0.1, 0.15, 0.2mm for depth of cut while each of the other two cutting variables were set at four levels, i.e. 80, 100, 120, 140 m/min for cutting speed and 0.05, 0.07, 0.09, 0.11mm/rev for feed rate. And there is totally 48 (3×4×4) combinations of turning conditions and they are all carried out in this study for completeness.

Hard material turning experiment set-up and its apparatus arrangement are shown in Fig.1. Here, tool flank wear and the roughness of the machined surface of the workpiece are measured through the toolmaker's microscope and the roughness measuring instrument, respectively after a surface layer removed from the workpiece during each cutting condition set, while the cutting noise deduced and cutting temperature during each surface layer workpiece removing of turning process were also detected via sound level meter and non-contact type of infrared thermometer on-line, respectively. The whole associated experimental flow procedures including the cutting performance relating parameter on-line detection and off-line measurements are shown in Figure 2.

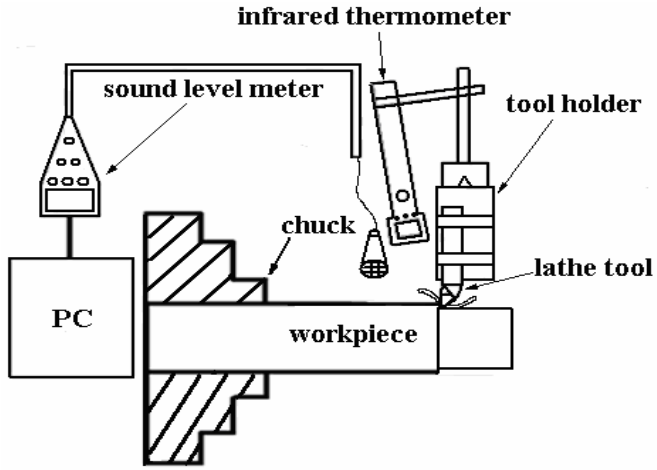

Figure 1 Schematic diagram of the turning experiment set-up

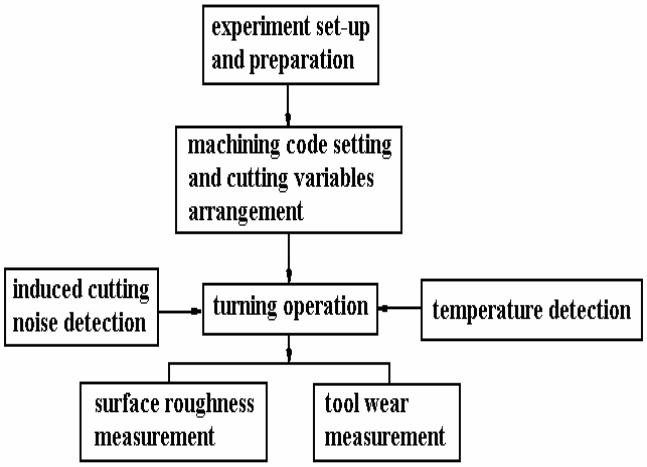

Figure 2 Flow chart for turning experiment

## 3. Abductive network synthesis and evaluation

Abductive network is a specific neural network. In an abductive network, a complex system can be decomposed into smaller, simpler subsystems grouped into several layers using polynomial function nodes. The polynomial network proposed by Ivakhnenko [14] is a group of methods of data handling (GMDH) techniques. These nodes evaluate the limited number of inputs by a polynomial function and generate an output to serve as an input to subsequent nodes of the next layer. The general polynomial function in a polynomial functional node can be expressed as follows:

$$y_0 = b_0 + \sum_{i=1}^{n} b_i x_i + \sum_{i=1}^{n}\sum_{j=1}^{n} b_{ij} x_i x_j + \sum_{i=1}^{n}\sum_{j=1}^{n}\sum_{k=1}^{n} b_{ijk} x_i x_j x_k + \cdots \quad (1)$$

where $x_i$, $x_j$, $x_k$ are the inputs, $y_0$ is the output and $b_i$, $b_{ij}$, $b_{ijk}$ are the coefficients of the polynomial functional nodes.

In this paper, several specific types of polynomial functional nodes are used in polynomial network to predict the cutting tool wear and surface roughness for precision mold turning. These polynomial functional nodes are named as normalizer(N), unitizer(U), white(W), single(S), double(D) and triple(T) nodes.

To build a complete abductive network, the first requirement is to train the database. The information given by the input and output parameters must be sufficient. A predicted square error (PSE) criterion is then used to automatically determine an optimal structure[15]. The principle of the PSE

criterion is to select the least complex yet still accurate network as possible. The PSE is composed of two terms; that is:

$$PSE=FSE+K_P \tag{2}$$

where *FSE* is the average square error of the network for fitting the training data and $K_P$ is the complex penalty of the network, shown as the following equation:

$$K_p = CPM \frac{2\sigma_p^2 K}{N} \tag{3}$$

where *CPM* is the complex penalty multiplier, *K* is a coefficient of the network, *N* is the number of training data to be used and $\sigma_P^2$ is a prior estimate of the model error variance.

**4. Results and discussion**

The relationship among surface roughness, cutting speed and feed rate under the depth of cut of 0.1mm is shown in Figure 3. Surface roughness is increased with increasing feed rate and almost increasing cutting speed comparably.

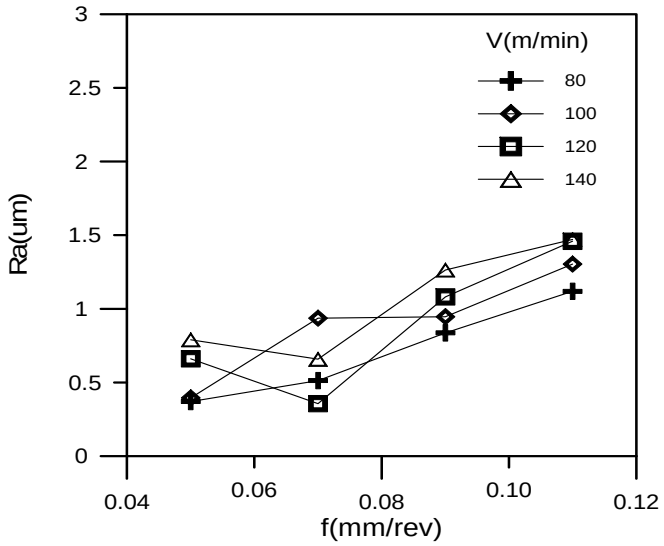


Figure 3 Relationship among surface roughness, cutting speed and feed rate under the depth of cut of 0.1mm

The relationship among surface roughness, depth of cut and feed rate under the cutting speed of 120m/min is shown in Figure 4. As expected, surface roughness is increased with increasing depth of cut.

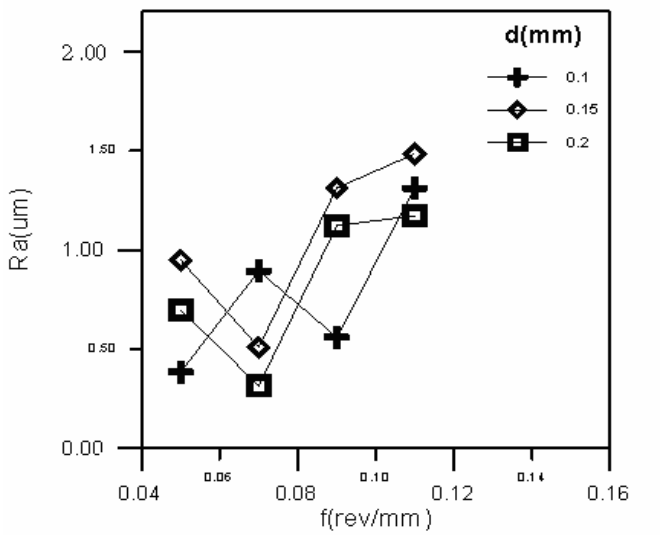

Figure 4 Relationship among surface roughness, depth of cut and feed rate under the cutting speed of 120m/min

The relationship among cutting temperature, cutting speed and feed rate under the depth of cut of 0.1mm is shown in Figure 5. The cutting temperature was measured through an infrared thermometer which was adjusted focusing on tool edge tip for its measurement during the turning process on-line. The maximum temperature is found locating around the primary cutting zone and its level detected is about 600℃ when the cutting tool edge was piled up the sufficient amount of chip. A large material removal rate produced depending on the higher value setting of the process parameters. Hence, the cutting temperature is increased as the feed rate, cutting speed and depth of cut is increased.

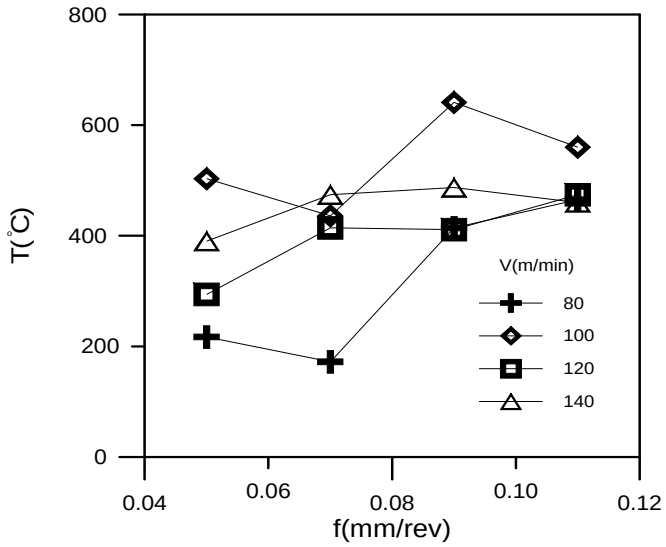


Figure 5 Relationship among cutting temperature, cutting speed and feed rate under the depth of cut condition of 0.1mm

Chip type is one of the important index for machining state judgment. In this study, cutting chip was collected after each surface layer removed from the workpiece in the turning experiment. There is much complex chip type exhibited during different cutting conditions in the experiment, which may be arranged and divided into 6 categories, A-F type. A to C chips belong to the continuous strip chip with different curly radii while D to E chips may be regarded as a discontinuous chip with different curly morphologies such as small c, segmented and spiral shapes, respectively.

（a）A type

（b）Btype

（c）C type

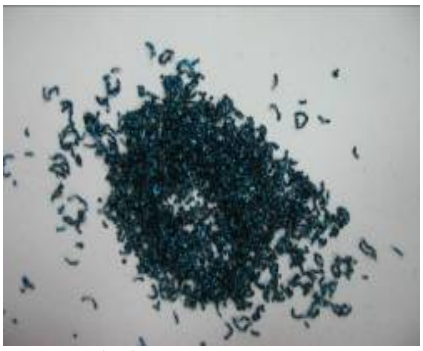

（d）D type

（e）E type

（f）F type

Figure 6 Various chip types collected from the turning experiment

The experiment results show that feed rate is the key factor affecting the surface roughness. The chips became segmented when feed rate is increased, which in turn causes the machined surface roughness having a big extent in variation. Type A and B chips as shown in 6(a) and 6(b) namely for this state, and the surface roughness associated with A type chip is also better than that of B type. Larger cutting depth deduces the cutting temperature to be higher and easily to form the D type chip. The high temperature is generated due to a great lot chip accumulated on the cutting edge when a great amount of materials removing from the workpiece. The temperature at the cutting tool tip rises subsequently and the purple and black chips were thus produced as shown in Figure 6(c) and 6(d). The chips shown in Figure 6(e) and 6(f) reflect the effect of the cutting speed change, when cutting speed is increased F type chip is likely to form, this is because of a tangle distortion phenomenon within chip resulting from the large cutting force acting on the chip. The relationship among surface roughness, cutting temperature and chip types is synthesized shown in Figure 7. As mentioned above, the cutting temperature may be measured appropriately through the chip being piled sufficiently up the cutting edge, the cutting temperature tends to be higher when the machined surface is rougher due to severe setting of different cutting conditions.

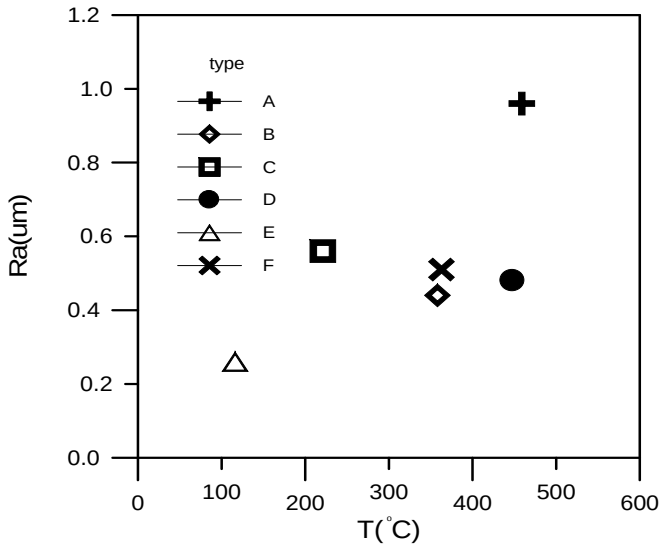


Figure 7 Relationship among surface roughness, cutting temperature and chip types

Based on the training database regarding to process variable combinations and their corresponding cutting tool wear obtained from the experiments, the abductive network can be developed for predicting the PCBN tool wear. A two-layer network shown in Figure 8 is built for predicting cutting tool wear under different high-speed machining conditions. The network shown in Figure 8 is created by 48 machining data sets as mentioned above, which is the optimal structure based on the principle of the predicted square error criterion and can be utilized to determine the tool wear under various combinations of process parameters in a continuous manner. The PSE deduced from the statistical synthesis is 3.854E-8.

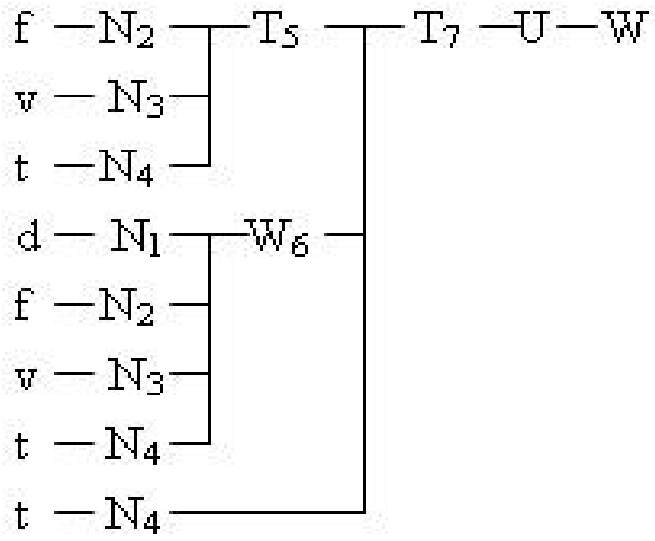


Figure 8 Abductive networks for predicting cutting tool flank wear

Cutting noise emitted during the cutting process taken from this experiment is mainly used to investigate how its magnitude and property related to the performance of precision mold machining and try to establish a relationship between noise and cutting performance. Cutting tool wear is one of the influential factor on cutting noise variation. When the cutting tool wear is big, the cutting edge getting blunt and the level of noise is raised. The noise more loudly indicating its tool wear is more serious. The machined surface roughness and dimensional accuracy are thus also worse after turning. In addition, cutting depth is also an affecting factor related to cutting noise. When cutting depth was set as large as 0.2mm, the level of noise is all kept at high value no matter what the feed rate and cutting speed change.

The level of noise all falls in a cope that human can be endured, and the tool wear approaches to zero and the workpiece surface roughness is very good when depth of cut was set as 0.1mm,.

## 5. Conclusion

In order to understand the superior characteristics of PCBN tool for hardened material cutting, to promote the performance and efficiency of precision mold manufacturing via the high speed machining technology, to investigate the wear mechanism of the tool and the quality of the machined surface. Mold steel workpiece materials and polycrystalline cubic boron nitride were used in this study as the workpiece and tool materials, respectively in the turning experiments for investigating the performance of precision mold manufacturing. After 48 set combinations of process variables all undertook in is study repeatedly, a better surface finish and lesser cutting tool wear may be obtained when the level of feed rate is set falling in 0.05-0.07mm/rev range. Similarly, a better surface finish near to grinding operation may be obtained when the level of cutting speed is set as 80m/min, with a surface roughness of Ra0.2-0.8μm. While, a good cutting performance is found when the level of depth of cut is set as smaller as possible such as 0.1 or 0.2mm in this study. From the above physical verifications, the grinding operation traditionally used for hardened material processing can be replaced by turning using PCBN tool due to its precision characteristics of machining.

## 6. References


[1] K. S. Neo, M. Rahman, X. P. Li, H. H. Khoo, M. Sawa, Y. Maeda, Performance evaluation of pure CBN tools for machining of steel, *J. Mater. Process. Technol.*, Vol.140 (2003) 326-331.

[2] X. J. Ren, R. D. James, E. J. Brookes, L. Wang, Machining of high chromium hardfacing materials, *J. Mater. Process. Technol.*, Vol.115 (2001) 423-429.

[3] X. J. Ren, Q. X. Yang, R. D. James, L. Wang, Cutting temperatures in hard turning chromium hardfacings with PCBN tooling, *J. Mater. Process. Technol.*, Vol.147 (2004) 38-44.

[4] W. Y. H. Liew, B. K. A. Ngoi, Y.G. Lu, Wear characteristics of PCBN tools in the ultra-precision machining of stainless steel at low speeds, *Wear*, Vol.254 (2003) 265-277.

[5] G. C. Benga, A. M. Abrao, Turning of hardened 100Cr6 bearing steel with ceramic and PCBN cutting tools, *J. Mater. Process. Technol.*, Vol.143-144 (2003) 237-241.

[6] H. Kato, K. Shintani, H. Sumiya, Cutting performance of a binder-less sintered cubic boron nitride tool in the high-speed milling of gray cast iron, *J. Mater. Process. Technol.*, Vol.127 (2002) 217-221.

[7] J. M. Zhou, H. Walter, M. Andersson, J. E. Stahl, Effect of chamfer angle on wear of PCBN cutting tool, *Int. J. Mach. Tools Manuf.*, Vol.43 (2003) 301-305.

[8] M. W. Cook, P. K. Bossom, trends and recent developments in the material manufacture and cutting tool application of polycrystalline diamond and polycrystalline cubic boron nitride, *Int. J. Refract. Metals Hard Mater*., Vol.18 (2000) 147-152.

[9] Antônio Maria de Souza Jr., Wisley Falco Sales, Sandro Cardoso Santos, Alisson Rocha Machado, Performance of single Si3N4 and mixed Si3N4+PCBN wiper cutting tools applied to high speed face milling of cast iron, *Int. J. Mach. Tools Manuf.*, Vol.45 (2005) 335-344.

[10] Z. Y. Wang, K. P. Rajurkar, M. Murugappan, Cryogenic PCBN turning of ceramic ($Si_3N_4$), *Wear*, Vol.195 (1996) 1-6.

[11] T. Kitagawa, A. Kubo and K. Maekawa, Temperature and wear of cutting tools in high-speed machining of Inconel 718 and Ti-6Al-6V-2Sn, *Wear*, Vol.202 (1997) 142-148.

[12] T. I. El-Wardany, E. Mohammed, M.A. Elbestawi, Cutting temperature of ceramic tools in high speed machining of difficult-to-cut materials, *Int. J. Mach. Tools Manuf.*, Vol.36 (1996) 611-634.

[13] G. Sutter, A. Molinari, L. Faure, J.R. Klepaczko, D. Dudzinski, An experimental study of high speed orthogonal cutting, *Trans. ASME, J. Manuf. Sci. Eng.*, Vol.120 (1998) 169-172.

[14] A. G. Ivakhnenko, Polynomial theory of complex system, *IEEE Trans.Syst.*, Vol.1 (1971) 364-378.

[15] A. R. Barron, Predicted square error: A criterion for automatic model selection, self-organizing methods in modeling: GMDH type algorithms, edited by Farlow, S. J. *Marcel-Dekker*, New York (1984)